Applied Catalysis B: Environmental 304 (2022) 120968

Contents lists available at ScienceDirect

Applied Catalysis B: Environmental

journal homepage: www.elsevier.com/locate/apcatb

Pulse pyrolysis of waste cooking oil over CaO: Exploration of catalyst deactivation pathway based on feedstock characteristics

Qiuhao Wu [a,1], Linyao Ke [a,1], Yunpu Wang [a,*], Nan Zhou [b], Hui Li [c], Qi Yang [a], Jiamin Xu [a], Leilei Dai [a,b], Rongge Zou [d], Yuhuan Liu [a], Roger Ruan [b]

[a] State Key Laboratory of Food Science and Technology, Engineering Research Center for Biomass Conversion, Ministry of Education, Nanchang University, Nanchang 330047, China
[b] Center for Biorefining and Department of Bioproducts and Biosystems Engineering University of Minnesota, 1390 Eckles Ave., St. Paul, MN 55112, USA
[c] School of Thermal Engineering, Shandong Jianzhu University, Jinan 250101 China
[d] Department of Biological Systems Engineering, Washington State University, Richland, WA 99354-1671, USA

ARTICLE INFO

Keywords:
Waste cooking oil
Free fatty acid
Pulse pyrolysis
CaO
Deactivation

ABSTRACT

Pulse pyrolysis was carried out to realize real-time monitoring of CaO catalyst deactivation and regeneration in the catalytic pyrolysis of waste cooking oil (WCO) and free fatty acids (FFAs) based on the pyrolysis characteristics of feed stocks. The high unsaturation of the feedstock decreases the initial decomposition temperature and reduces the content of oxygen-containing compounds. CaO catalyst was completely deactivated after several times of pulse pyrolysis. During the pyrolysis of WCO, the catalytic activity of CaO did not recover after the pause of pulse pyrolysis. However, the catalytic activity all recovered during the pyrolysis of FFAs, but the rate of deactivation was accelerated. A large amount of $Ca(OH)_2$ and $CaCO_3$ were detected in the deactivated catalyst, and soluble coke was not detected. The research suggested that the change of crystal phases and agglomeration were the vital cause that impact the CaO catalyst stability.

1. Introduction

The development of renewable resources to alleviate the excessive consumption of fossil energy in recent years is a research hotspot [1]. It is of positive significance to achieve carbon neutrality conversion of biomass to produce green and sustainable energy substances to replace fossil energy [2]. Edible oil is an indispensable ingredient in daily life, and a large amount of waste oil is produced in the process of production and consumption. China alone produced 66.55 million tons of major edible oil and consumed 36 million tons of major vegetable oil in 2019 [3]. Fast pyrolysis is one of the most promising technologies for the thermal conversion of biomass to liquid fuel due to its high liquid yield [4].

Different from lignocellulosic biomass, lipid biomass has small molecular weight and simple composition. The main components of lipid biomass are triglycerides and a small amount of free fatty acids (FFAs), which means that the preparation of hydrocarbons from lipid biomass requires only the selective removal of the ester group in triglycerides and the carboxyl group in FFAs. With the presence of catalysts, the oxygen from lipid biomass could be removed in the form of H_2O, CO, CO_2, and other small molecule oxygen-containing compounds through decarboxylation [5], decarbonylation [6], ketonization [7], aromatization [8], and cracking. Commonly used catalysts include zeolite catalysts (ZSM-5, MCM-41, HY, and et al.), activated carbon catalysts (commercial and homemade), metal oxide catalysts (CaO, MgO, SrO, ZrO_2, CoO, and et al.), and the other composite catalysts. Catalyst fast pyrolysis can significantly reduce the content of oxygen-containing compounds and improve the selectivity of some expected components in bio-oil. As shown in our previous study [7], the total content of benzene, toluene, xylenes, ethylbenzene, and styrene obtained from the pyrolysis of waste cooking oil (WCO) over CaO and HZSM-5 was up to 702.2 mg/ml. The study conducted by Xu et al. [9] showed the pyrolysis of waste oil with Ni/HZSM-5 as catalyst could obtain aviation bio-fuel with a high yield of over 60%. In addition, many studies have shown that the catalytic pyrolysis of waste oil or other triglycerides can obtain high-quality hydrocarbon products. For example, γ-Al_2O_3 catalyzed the conversion of sunflower oil to bio-fuel close to standard fossil fuel [10], and Zn/ZSM-5 catalyzed the conversion of canola oil methyl ester to

* Correspondence to: MOE, Engineering Research Center for Biomass Conversion, Nanchang University, 235 Nanjing East Road, Nanchang, Jiangxi 330047, China.
E-mail address: wangyunpu@ncu.edu.cn (Y. Wang).
[1] These authors contributed equally

https://doi.org/10.1016/j.apcatb.2021.120968
Received 18 August 2021; Received in revised form 23 November 2021; Accepted 24 November 2021
Available online 26 November 2021

aromatics at a yield of 42.6% [11].

Notably, catalyst deactivation is always inevitable and is a bottleneck of the catalytic fast pyrolysis technology [12]. The causes of catalyst deactivation include coking [13], pore structure collapse [14], poisoning [12,15], sintering [16], and agglomeration [17]. At present, the research mainly focuses on the deactivation of zeolite catalysts and their derivatives in the catalytic pyrolysis of lignocellulosic biomass. The deactivation of alkaline metal oxides during the catalytic pyrolysis of lipid biomass is different from that of zeolite catalysts.

Fan et al. [18] studied the deactivation of HZSM-5 catalyst during the pyrolysis of biomass. Thermogravimetry (TG) analysis of used catalysts showed two types of coke deposited on catalysts. One was oxygenated coke and the other was graphite-like coke. And further studies indicated that coke deposited on the catalyst were related to the acid sites of catalyst, and precursors include aromatic species, aliphatic hydrocarbons, and carbonyl compounds. For catalysts containing metals or metal oxides, such as Ni/Al_2O_3 [19,20], $Ni/MgAl_2O_4$ [20], and Ni-Ce/Mg-Al [21], metal sintering is also a cause of deactivation. The hydrothermal treatment of ZSM-5 showed that removal of aluminum species from ZSM-5 structure was a cause of deactivation [22], and the generation of hot water vapor during biomass pyrolysis was inevitable. Compare with acidic catalysts, alkaline earth metal oxides (such as CaO, MgO, and SrO) coking deactivation were alleviated due to lack of acid sites and thus the weak aromatization ability. Previous studies showed alkaline earth metal oxides increased CO_2 production rather than H_2O, which was helpful in increasing the heating value due to the retention of hydrogen atoms and removing of oxygen atoms in bio-oil [16]. And there are few studies focusing on the causes of the deactivation of metal oxides during the catalytic pyrolysis of lipid biomass especially for the real-time monitoring. Understanding the deactivation process and mechanisms of metal oxides during the pyrolysis of lipid biomass can provide direction for the development of subsequent catalysts. In this way, the application of metal oxides in lipid biomass pyrolysis can be promoted and the basic research data can be provided for the high value utilization of lipid biomass pyrolysis.

The deactivation of commercial calcium oxide (CaO) catalyst during the catalytic fast pyrolysis of WCO was monitored in real-time in this paper. The characterization of WCO and its main fatty acid composition was studied first by TG and Py-GC/MS. The change of catalytic activity of CaO catalyst during the intermittent pyrolysis of WCO was monitored in real-time by Py-GC/MS through pulse pyrolysis. The initial catalytic activity and the change of catalytic activity of CaO catalyst under different FFAs were studied. Also, FT-IR, XRD, and TG analysis of the used CaO were studied to investigate the causes of deactivation. In addition, the deposition of organic species on the surface of the used CaO was studied by solvent extraction and GC/MS analysis. The deactivation pathways of CaO catalyst in the catalytic pyrolysis of WCO and FFAs were speculated.

2. Materials and methods

2.1. Materials

WCO was obtained from fresh edible oil (Yihai Kerry Oils and Foodstuffs Co. Ltd. Nanchang, China) after being used to fry French fries and filtered, then stored in a refrigerator at 4 °C for further experiments. The fatty acid composition and FFAs content of WCO were shown in Table 1. The FFAs were directly used without any treatment during the experiments, which included stearic acid (98%, CAS: 57-11-4, Shanghai Aladdin Biochemical Technology Co., Ltd.), oleic acid (AR, CAS: 112-80-1, Shanghai Aladdin Biochemical Technology Co., Ltd.), and linoleic acid (>95.0% for GC, CAS: 60-33-3, Shanghai Aladdin Biochemical Technology Co., Ltd.). The catalyst used in this study was the commercial calcium oxide (CaO, CAS: 1305–78–8, Xilong Scientific Co., Ltd.) calcined at 900 °C for 2 h. The solvent used for the possible organics deposited on the used CaO dissolving treatment is dichloromethane (CH_2Cl_2, CAS: 75-09-2, Macklin).

Table 1
The fatty acid composition and FFAs content of WCO. FFAs: Free fatty acids, WCO: Waste cooking oil.

WCO characteristics		
Fatty acid (wt%)	Palmitic acid (16:0)	11.434 ± 0.040
	Stearic acid (18:0)	4.974 ± 0.072
	Oleic acid (18:1)	33.698 ± 0.306
	Linoleic acid (18:2)	49.130 ± 0.362
	Others	0.765 ± 0.246
Free fatty acid content (wt%)		0.121 ± 5e-4

2.2. Feedstock characterization

2.2.1. Composition analysis

The fatty acid composition of WCO was determined by GC-MS using fatty acid methyl ester as the test sample prepared by methyl esterification. The FFAs in WCO was determined by titration method. Each analysis test was replicated at least three times.

2.2.2. TG analysis

To investigate the thermal behavior of the FFAs, sample were heated from room temperature to 800 °C at 20 °C/min under 100 ml/min of high-purity N_2 using a thermogravimetric analyzer (TG, DTG-60H, Shimadzu Co., Ltd). A corundum crucible with a lid was used during the analysis.

2.3. Catalyst characterization

2.3.1. TG and FT-IR analysis

The fresh CaO and the used CaO were analyzed by TG and Fourier Transform infrared spectroscopy (FT-IR, Nicolet iS5, Thermo Fisher) to determine the contents of $Ca(OH)_2$, $CaCO_3$ and other possible organics. During the TG analysis, catalysts were heated from the room temperature to 1000 °C at 10 °C/min under 50 ml/min of air. During the FT-IR analysis, the spectral range of FTIR spectrometer, the resolution, and the scanning times were set to 4000–400 cm^{-1}, 4 cm^{-1}, and 32 times, respectively.

2.3.2. XRD analysis

X-ray diffraction (XRD, Rigaku Smartlab, Japan) analysis was performed to further determine the phase composition of the used CaO, with Cu Kβ radiation (1.3922 Å, 40 KV × 30 mA) over a 2θ range of 10–90° and a scanning speed of 4 °/min.

2.3.3. Particle size and morphology analysis

Particle size of fresh CaO and used CaO was analyzed by Mastersizer 2000 (Malvern, UK). Morphology analysis of fresh CaO and used CaO was conducted by scanning electron microscopy (SEM, Sigma 500, Zeiss, Germany).

2.3.4. Extract analysis

To analyze the possible organics deposited on the used CaO, the catalyst dissolved in CH_2Cl_2 was vibrated by ultrasonic treatment for 4 h and then held for 48 h, and finally the collected extract was analyzed by gas chromatograph-mass spectrometer (GC-MS, 7890B-7000D, Agilent Technology Co., Ltd) [18].

2.4. Catalytic pyrolysis test

The catalytic pyrolysis test was carried out in a pyrolyzer (Py, 5200HPR, CDS Analytical Inc.) with trap mode coupled with GC-MS (GC-MS, 7890B-7000D, Agilent Technology Co., Ltd), and the device schematic diagram was shown in Fig. 1. The same catalyst was used 50 times under pulse pyrolysis conditions while the feedstock was replaced

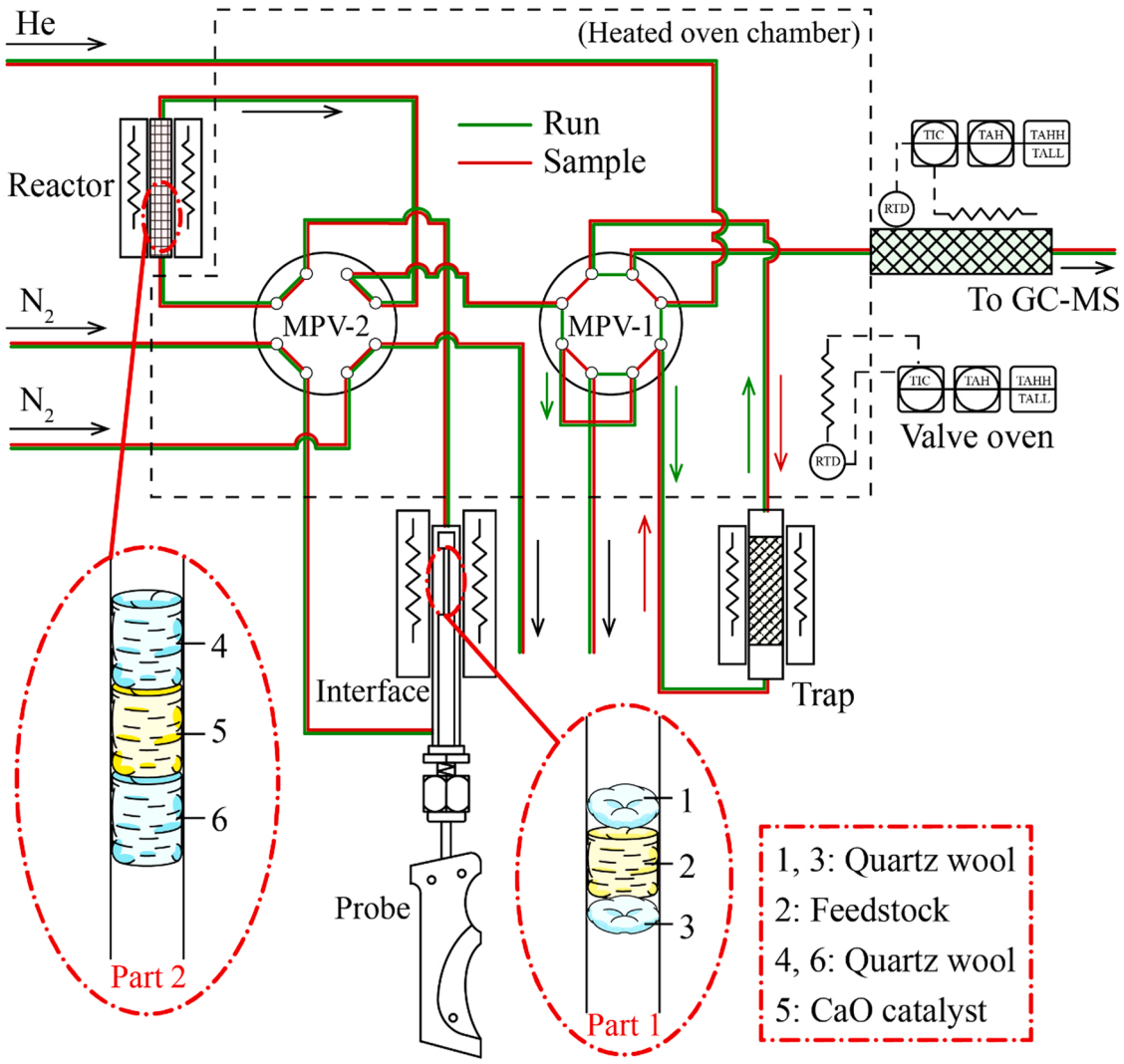

Fig. 1. The device schematic diagram of Py-GC/MS.

each experimental run. For each experimental run, the weight of the feedstock (WCO, stearic acid, oleic acid, or linoleic acid) was strictly controlled at 0.40 ± 0.02 mg using a microbalance. Similarly, the weight of the catalyst, CaO, was controlled at 100 ± 5 mg. The feedstock was loaded into the quartz tube (25*mm* × 1.9*mm*) in the following order: quartz wool, feedstock, quartz wool (Fig. 1, part 1). The catalyst was loaded into a special catalytic reactor with the same placement mode (Fig. 1, part 2). The sample quartz tube was inserted into the platinum coil of the probe rod and underwent fast pyrolysis, the pyrolysis vapor firstly flowed through the catalytic reactor for catalytic reforming and then was adsorbed by the trap under 50 ml/min of high-purity N_2. During 300 °C of high-temperature desorption for 2 min, the pyrolysis products were directly transferred to GC-MS by a transfer line under high-purity N_2 to complete the online analysis. The detailed operating conditions of Py-GC/MS were shown in Table 2. In particular, during the 50 times pulse pyrolysis, the pyrolysis experiments were intermittently interrupted several times without sample injection, however, the catalyst was still at 500 °C in the N_2 atmosphere with the flow rate of 50 ml/min.

Table 2
Operating conditions of Py-GC/MS.

Operating conditions of Py		Operating conditions of GC/MS	
Heating rate	20 °C/ms	Chromatographic column	HP-PONA capillary column (50 m × 0.200 mm × 0.50 μm)
Pyrolysis temperature	650 °C	Injector temperature	280 °C
Pyrolysis time	30 s	Split ratio of injector	50:1
Catalytic reactor temperature	500 °C	Heating program	40 °C - 2 min - 5 °C/min - 280 °C/min - 3 min
Adsorbent temperature of trap	50 °C	Carrier gas type	Ultra-purity helium
Desorption temperature of trap	300 °C	MS electron ionization (EI) mode	m/z = 30–550, ionization voltage = 70 eV
Desorption time of trap	2 min	Ion source temperature	230 °C
Valve box temperature	280 °C	Quadrupole temperature	150 °C
Transfer temperature	280 °C	Search speclrum library	NIST MS library database
Carrier gas type	Ultra-purity nitrogen		

3. Results and discussion

3.1. Pyrolysis characterization of feedstock

In order to better study the deactivation of CaO catalyst in the pyrolysis process of WCO, the pyrolysis characterization of WCO and its main fatty acid composition was studied first. Fig. 2 showed the TG and DTG analysis of WCO and its main fatty acid composition, and DTG analysis was given by taking the derivative of TG analysis. It can be seen that after a certain temperature, the weight loss all reached 100%, indicating that the char yield can be ignored during pyrolysis of WCO and FFAs at high temperature [7]. Peak weight loss temperature of WCO with the range of 300–500 °C was significantly higher than that of FFAs within 150–400 °C. The study of Qiao et al. [23] showed that palm oil pyrolysis was in a narrower temperature range of 385.2–488.4 °C, and the fast pyrolysis occurred at 440 °C according to the TG analysis. The molecular weight of WCO was about three times that of FFAs, and the intermolecular force is stronger. Table 1 showed that WCO contained very little FFAs, which were mainly triglycerides. Also, there was an interesting phenomenon that the weight loss rate of unsaturated FFAs (oleic acid and linoleic acid) decreased in the high temperature region, which could be clearly found from DTG analysis. There were two or more decomposition peaks for unsaturated FFAs (oleic acid and linoleic acid), while there was only one decomposition peak for saturated FFAs (stearic acid) and WCO. This was because both C-C double bond and COOH were electron-withdrawing groups, leading to a decrease in the bond dissociation energy of the C-C bond outside of the two groups, which was more liable to fracture at low temperature, and the C-C bond between the two groups was more stable than that of saturated FFAs. This can also explain that the initial decomposition temperature of unsaturated FFAs was lower and the decomposition temperature range was wider. The presence of C-C double bonds decreased the pyrolysis temperature [24]. The maximum rate of mass loss from high to low in order was stearic acid, oleic acid, WCO, and linoleic acid. The presence of C-C double bonds promoted the cracking of long carbon chain of FFAs [25]. This phenomenon was also related to the different of C-C bond dissociation energy in FFAs molecules. According to the TG analysis, pyrolysis temperature was set to 650 °C in the subsequent Py-GC/MS experiment.

Py-GC/MS analysis was conducted to learn more about the pyrolysis characterization of WCO and FFAs. As shown in Fig. 3, deoxygenation occurred during the pyrolysis, the maximum relative content of oxygen-containing compounds reached 43.28%, which was obtained during the pyrolysis of stearic acid. With the increase of unsaturation of FFAs, the relative content of oxygen-containing compounds also decreased

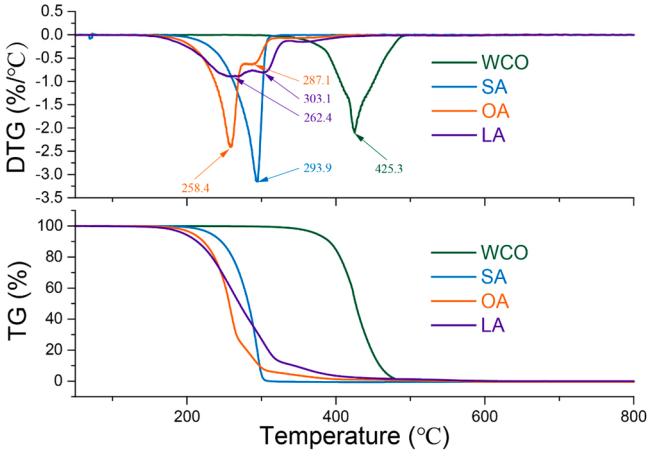

Fig. 2. TG and DTG analysis of WCO and FFAs. TG: Thermogravimetric, DTG: Derivative thermogravimetry, WCO: Waste cooking oil, SA: Stearic acid, OA: Oleic acid, LA: Linoleic acid.

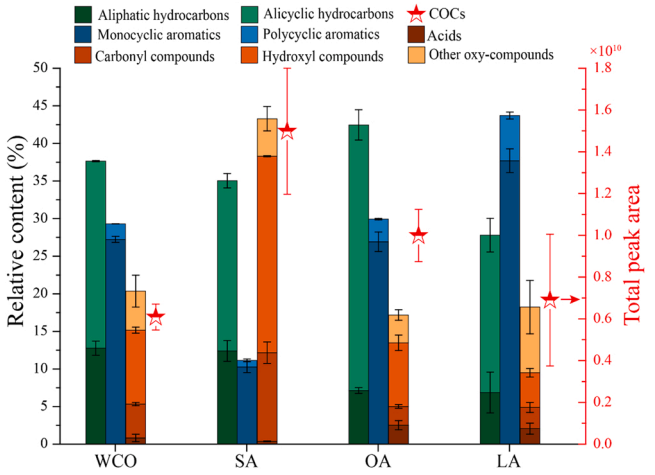

Fig. 3. Py-GC/MS analysis of WCO and FFAs. WCO: Waste cooking oil, SA: Stearic acid, OA: Oleic acid, LA: Linoleic acid, COCs: Condensable organic compounds, oxy-compounds: oxygen-containing compounds. The total peak area of COCs was obtained from 1 mg feedstock, which was obtained by conversion.

gradually, and the lowest value was 17.19% during oleic acid pyrolysis. And the relative content of oxygen-containing compounds during linoleic acid pyrolysis was 18.22%. During the pyrolysis of fatty acids, the C-C double bond from the feedstock will be preserved, and a new C—C double bond will be formed [26]. It was inferred those alkanes and olefins produced during linoleic acid pyrolysis could promote the deoxygenation of oxygen-containing compounds from linoleic, so that oxygen-containing compounds from linoleic acid pyrolysis was the lowest content. At the same time, the olefins produced by pyrolysis will undergo cyclization and aromatization at high temperatures, even in the absence of catalysts [25]. Therefore, the content of aromatic hydrocarbons in the products from high to low was linoleic acid, oleic acid, and stearic acid, while the WCO was between oleic acid and linoleic acid. And the highest was exceeding 45%. This was because more olefins were produced during the pyrolysis of linoleic acid. There was a very interesting phenomenon that in the pyrolysis of stearic acid, a large number of long chain primary alcohols (C>10) were detected in condensable organic compounds (COCs), but not found in the pyrolysis products of oleic acid and linoleic acid. On the one hand, carboxyl compounds were probably reduced by hydrogen which can be produced by the reaction of CO with H_2O ($CO + H_2O = CO_2 + H_2$) [27] or by other reactions [28] to form hydroxyl compounds. In some reported studies, H_2 has been detected in gas products [28,29]. On the other hand, it was speculated that the free radical reaction occurred in the pyrolysis process, resulting in the generation of many long carbon chain hydrocarbon free radicals and carboxyl radicals, and chain termination reaction occurred between the two radicals to form short carbon chain carboxylic acids. At the same time, hydrogen radicals from the pyrolysis process attacked these carboxylic acids, and converted them to primary alcohols. Or the hydrogen radicals attacked the carboxyl radicals first to form the hydroxyl radicals, then termination reaction occurred between hydroxyl radicals and hydrocarbon free radicals to form primary alcohols. Hydrocarbon free radicals [30,31], carboxyl radicals [32], hydrogen radicals [31,33], hydroxyl radicals [33], and other radicals [34] have been reported in previous studies to support this hypothesis. CH_4, C_2H_4, and C_3H_8 were also detected in pyrolysis gas, indicating the cracking of long carbon chains in the pyrolysis process [35]. Therefore, many alcohols with carbon number smaller than 18 were found in the product. For unsaturated FFAs, C-C double bonds existed in the product, which were from the feedstock itself and the decarboxylation process [25], and cyclization and aromatization can occur at high temperature, resulting in the increase of the content of cycloalkanes, cycloolefins, and aromatic

hydrocarbons in the product.

3.2. Pyrolysis with CaO catalyst

After learning about the pyrolysis characterization of WCO and its main fatty acid composition, the change process of catalytic characteristics of CaO catalyst in WCO and FFAs was studied sequentially. In this section, the catalytic pyrolysis of three kinds of FFAs (stearic acid, oleic acid, and linoleic acid) and WCO were carried out in a series of 50 times of pulse pyrolysis with CaO catalysis.

3.2.1. Initial catalytic activity of CaO

The initial catalytic activity of CaO during the pyrolysis of WCO and FFAs was studied for the comparison of pyrolysis with or without catalyst. The percentage values on the lines shown in Fig. 4 represented the decline rates of the relative content of corresponding compounds, which were calculated according to the following formula

$$R_X = \frac{A_X - B_X}{A_X} \bullet 100\%$$

R_X, A_X and B_X represented the decline rate of the relative content of X, the relative content of X without catalysis, and the relative content of X with CaO catalysis, respectively. Overall, with CaO catalysis, all the oxygen-containing compounds decreased to varying degrees. From the perspective of feedstock type, the decline of the relative content of oxygen-containing compounds in FFAs was more obvious than that of WCO. At the same time, for FFAs, the relative content of oxygen-containing compounds was lower with catalytic pyrolysis mode due to the more double bonds existed in the feedstock. The presence of C-C double bonds in the products promoted deoxygenation not only in the absence of catalyst, but also under the condition of catalytic pyrolysis [36]. Fig. 4 showed that the presence of CaO promoted the deoxygenation of hydroxyl compounds and carbonyl compounds. The result was different from previous studies, which reported that CaO, as a type of alkaline-earth metal oxide, can promote the deoxygenation of carboxyl compounds to produce ketones [37]. However, it has been also reported that CaO can reduce the content of phenolics in bio-oil during oakwood pyrolysis [38], which was consistent with the conclusion of this paper. This indicates that the deoxygenation activity of CaO is not only influential for carboxyl compounds, but also for hydroxyl compounds and carbonyl compounds. Monocyclic aromatics were the main components of COCs during the catalytic pyrolysis with CaO except for stearic acid, of which the components were mainly aliphatic hydrocarbons. This indicates that the main products of hydroxyl compounds catalyzed by CaO are aliphatic hydrocarbons, but the increase of monocyclic aromatics was not obvious. There is a significant relationship between the content of olefins in the intermediate products and the content of monocyclic aromatics in the final products.

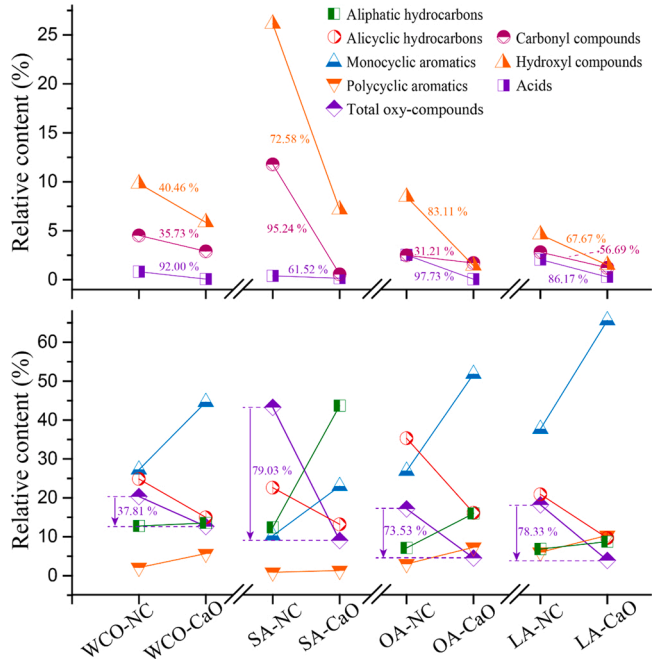

Fig. 4. The comparation of pyrolysis of WCO and FFAs with or without catalyst. WCO-NC: WCO pyrolysis without catalyst, WCO-CaO: WCO pyrolysis with CaO catalyst, SA-NC: Stearic acid pyrolysis without catalyst, SA- CaO: Stearic acid pyrolysis with CaO catalyst, OA-NC: Oleic acid pyrolysis without catalyst, OA-CaO: Oleic acid pyrolysis with CaO catalyst, LA-NC: Linoleic acid pyrolysis without catalyst, LA-CaO: Linoleic acid pyrolysis with CaO catalyst.

3.2.2. Pulse pyrolysis with CaO catalyst

In this section, the recovery of catalyst activity with intermittent sample injection in continuous production process was simulated randomly. The composition of COCs was real-time monitored during the experiments. Figs. 5–8 showed the real-time monitoring results of the composition of COCs during the pulse pyrolysis of WCO, stearic acid, oleic acid, and linoleic acid, respectively. Each red dotted arrow in the figures represented a pulse pyrolysis cycle, the red bolded short line represented the pause of pulse pyrolysis experiments, and the number in the outermost ring represented the total times of pulse pyrolysis experiments. The dotted circles within the black circles represented the relative content of some compounds without catalysis. In the figures, the larger the circle diameter was, the higher the compound content was. Catalyst activity discussion in this section is based on the content of hydroxyl compounds.

As shown in Fig. 5, CaO catalyst was completely deactivated after seven times of pulse pyrolysis. This was true both in terms of the relative content of alicyclic hydrocarbons and in terms of the relative content of oxygen-containing compounds or aromatics. During the 50 times pulse pyrolysis, the pyrolysis experiments were all paused over 10 h when the total pulse pyrolysis times were 13, 27, and 38, respectively. And the CaO catalyst was kept in the nitrogen atmosphere at 500 °C. However, no significant improvement of the catalyst activity was observed at the beginning of the next pulse pyrolysis cycle, when the composition of COCs was very similar to that under non-catalysis condition. The results of this study were consistent with the results of Yi et al. [17] that the CaO catalyst showed irreversible deactivation after 10 regeneration-recycles. In general, catalyst deactivation included reversible deactivation and irreversible deactivation types [39,40]. The study of Yi et al. [17] showed that irreversible deactivation existed during the catalytic pyrolysis of lignocellulosic biomass. Then it was speculated that there was also an irreversible deactivation process in the pyrolysis process of lipid biomass. Detailed analysis about the deactivation of CaO during the pulse pyrolysis of WCO are discussed in Section 3.3 of this paper.

In order to better explore the influence of feedstock characteristics on the deactivation and regeneration of CaO catalyst during the process of catalytic pyrolysis of lipid biomass, the deactivation of CaO catalyst during the catalytic pyrolysis process of FFAs was studied sequentially in this section. In terms of deoxygenation capacity (Figs. 6B, 7B, and 8B), the deactivation of CaO catalyst during the catalytic pyrolysis of FFAs was significantly different from that of WCO. First of all, the first complete deactivation time of CaO catalyst in the process of catalytic pyrolysis of FFAs was longer than that of WCO. Secondly, the catalytic activity of CaO catalyst was improved to varying degrees after each pause. During the pulse pyrolysis of stearic acid, the catalyst activity recovered to the initial activity after the intermittently interrupted without sample injection. During the pyrolysis of oleic acid and linoleic acid, the catalyst activity recovered after the intermittently interrupted without sample injection, but the activity was always lower than the initial activity. It was speculated that the deoxygenation pathways of WCO and FFAs were different during catalytic pyrolysis. The specific causes of deactivation were discussed in the next section. According to

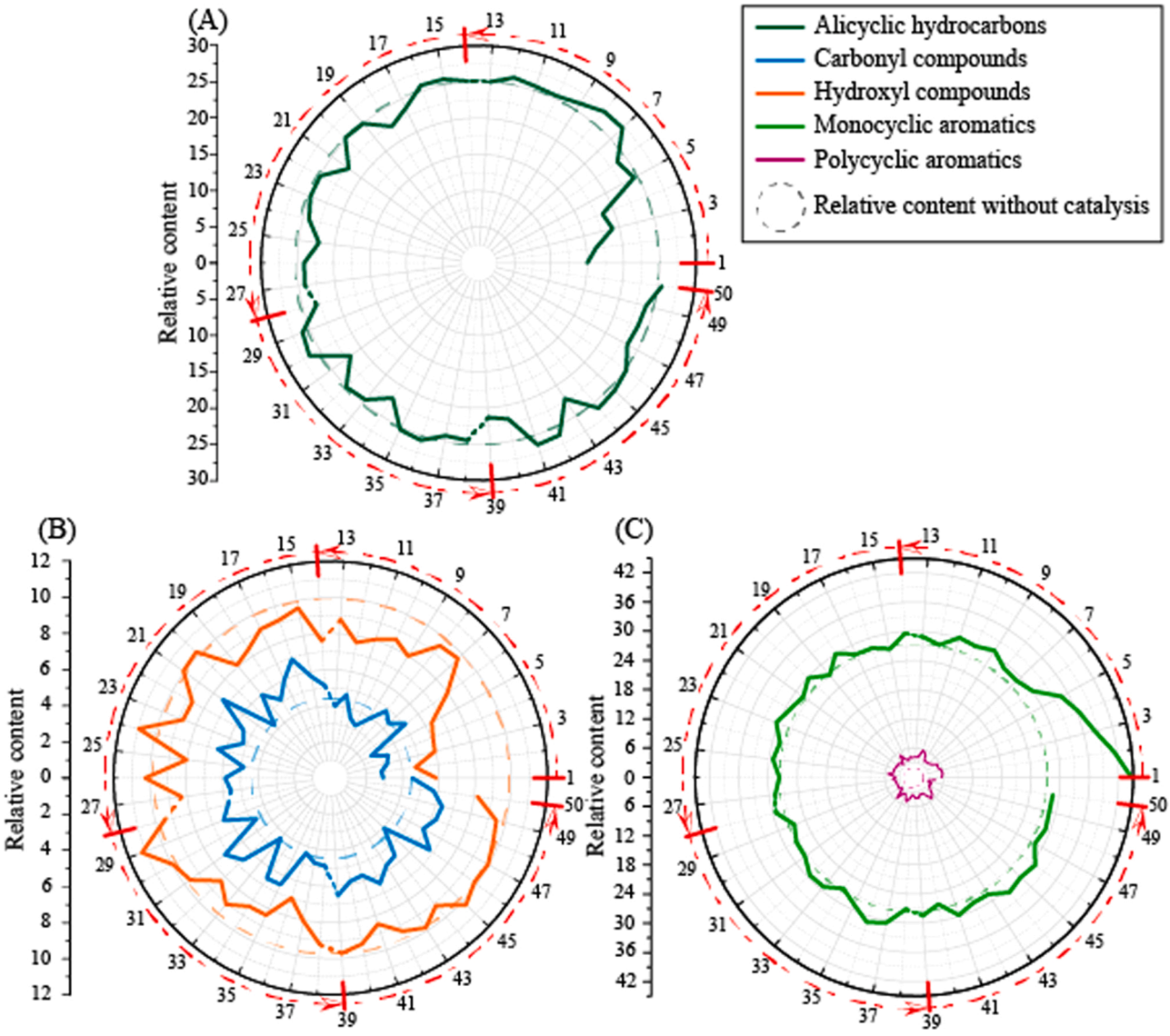

Fig. 5. The composition of condensable organic compounds during pulse pyrolysis of WCO.

the content of the main oxygen-containing compounds in the COCs, the regenerated catalyst was rapidly deactivated compared with the fresh CaO catalyst. And the rate of deactivation increased with the increase of total pulse pyrolysis times, which indicated that irreversible deactivation occurred during pyrolysis. Sintering of CaO was inevitable in the process of catalytic pyrolysis [41]. The first deactivation time of CaO catalyst during the pulse pyrolysis was stearic acid, oleic acid, and linoleic acid in descending order. According to the oxygen-containing compounds composition with non-catalysis (Fig. 4), it was speculated that the acids produced during pyrolysis stage had a significant influence on the deactivation of CaO catalyst. There are two important pathways of acids decarboxylation with CaO catalysis [42]. The first one is decarboxylation via the formation of CO_2 without the formation of $CaCO_3$, which takes place on the surface of CaO (pathway I). And the other is decarboxylation via the formation of calcium salts first, and then the calcium salts are decomposed into hydrocarbon and $CaCO_3$ (pathway II). The exact reaction pathway is determined by the alkalinity of CaO catalyst. A stronger alkalinity leads to pathway I, while a weaker alkalinity drives the reaction towards pathway II. Strong alkalinity promoted the deoxygenation of acids, but also the formation of $CaCO_3$.

In terms of the change of aromatics content in COCs (Figs. 6C, 7C, and 8C), the deactivation rate was slower than that in terms of the change of oxygen-containing compounds. Even after many times of repeated pulsed pyrolysis, the content of monocyclic aromatics with CaO catalyst fluctuated slightly above the content without catalysis. CaO catalyst also exhibited Lewis acidity during the catalytic process, which was provided by the Ca^{2+} [43,44]. The Lewis acidity of the catalyst was closely related to its aromatization ability [45]. However, the content of polycyclic aromatics (Figs. 6C–8C) was maintained at a relatively low level, which was because basic sites of CaO catalyst inhibited the further formation of polycyclic aromatics and coke [46,47]. Inhibiting catalyst coking reduced the coverage of acid sites in CaO catalyst, which explained the slower deactivation rate of aromatization. Well regeneration performance of catalyst in terms of aromatization ability indicated that the small amount of coke on CaO catalyst surface was easy to decompose at high temperature. Previous studies showed that there were two types of coke on the catalyst, one was oxygenated coke (type I), and the other was graphite-like coke (type II) [18]. The decomposition temperature of type I was lower than that of type II, which was 300–600 °C. Detailed analysis of coke formation on the CaO catalyst was studied in the next section.

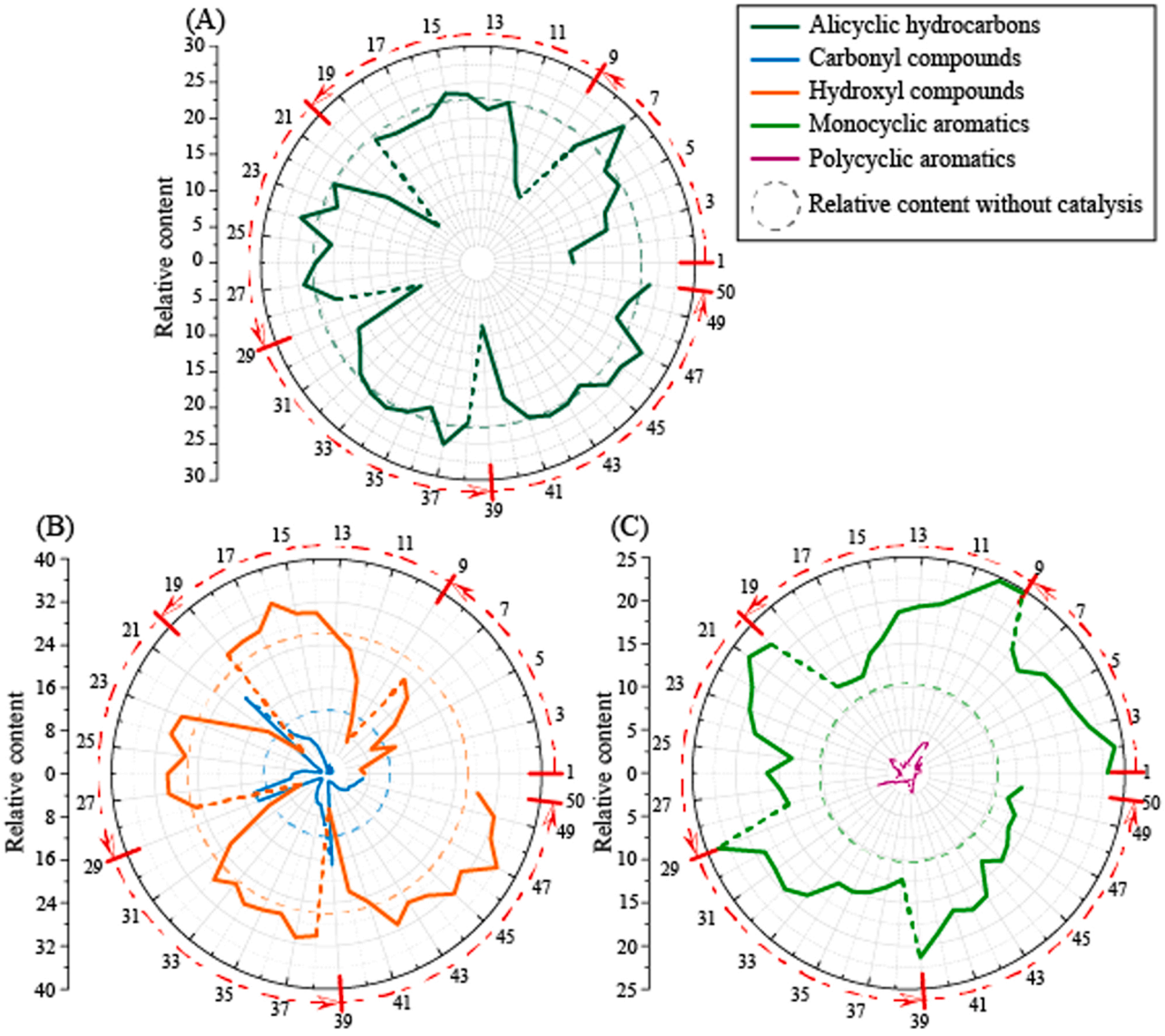

Fig. 6. The composition of condensable organic compounds during pulse pyrolysis of stearic acid.

3.3. Deactivation analysis of catalysts

Detailed analysis of CaO catalyst after 50 times of pulse pyrolysis was studied in this part. Particle size and SEM analysis of catalysts were conducted to analysis the change of particle size and morphology of used catalysts firstly. FT-IR and XRD analyses were used to qualitatively analyze CaO catalyst. TG and DTG analyses were used for further qualitative and quantitative analysis of the catalyst. Then the organic composition on the CaO catalyst was analyzed by GC/MS. Finally, detailed analysis of deactivation pathway was discussed.

The particle size distribution of fresh and used catalyst were showed in the Supplement data (Table S1). The D50 (median particle size) of Origin-CaO, WCO-CaO, SA-CaO, OA-CaO, and LA-CaO were 6.819 μm, 9.239 μm, 9.844 μm, 11.726 μm, and 12.340 μm, respectively. Compared with Origin-CaO catalyst, the D50 of all used-catalyst particle sizes increased, indicating that different degrees of agglomeration occurred after recycling of CaO catalyst. Studies showed that the agglomeration of CaO catalyst was a vital cause of CaO deactivation [48]. As shown in Fig. S1, SEM images confirmed the agglomeration of used catalyst. Agglomeration is a dynamic and continuous process during the pulse pyrolysis. Agglomeration proceeded slowly at first, which was not enough to cause the complete deactivation of catalyst. Therefore, the catalyst activity could be partially recovered after regeneration. SA-CaO has the lowest degree of agglomeration, so its catalytic activity can be almost completely recovered to the initial activity after regeneration. However, for OA-CaO and LA-CaO, the agglomeration effect is more serious, so the catalyst activity is only recovered to a limited degree after the regeneration process. Fig. 9 showed the FT-IR analysis of the original CaO and used CaO. As shown in Fig. 9A, 3638 cm^{-1} represented the stretching vibration of O-H in $Ca(OH)_2$ with a strong and sharp peak, 1420 cm^{-1} represented antisymmetric stretching vibration of CO_3^{2-} in $CaCO_3$ with a strong and wide peak, 876 cm^{-1} represented the out-of-plane bending of CO_3^{2-} in $CaCO_3$ with a weak peak, while 719 cm^{-1} represented the in-plane bending of CO_3^{2-} in $CaCO_3$ with a weak peak. FT-IR analysis showed that there were a higher content of $Ca(OH)_2$ and a lower content of $CaCO_3$ in WCO-CaO. There was a large amount of glycerol structure in the WCO, and a certain amount of H_2O generated during the pyrolysis process [50]. However, FFAs were more easily deoxygenated in the form of CO_2 during the catalytic pyrolysis. The oxygen atoms in WCO are mainly converted into CO, CO_2 and H_2O during the pyrolysis of WCO through decomposition of triglyceride and decarboxylation and ketonization of free fatty acids [51]. The oxygen atoms in FFAs are mainly converted into H_2O and CO_2

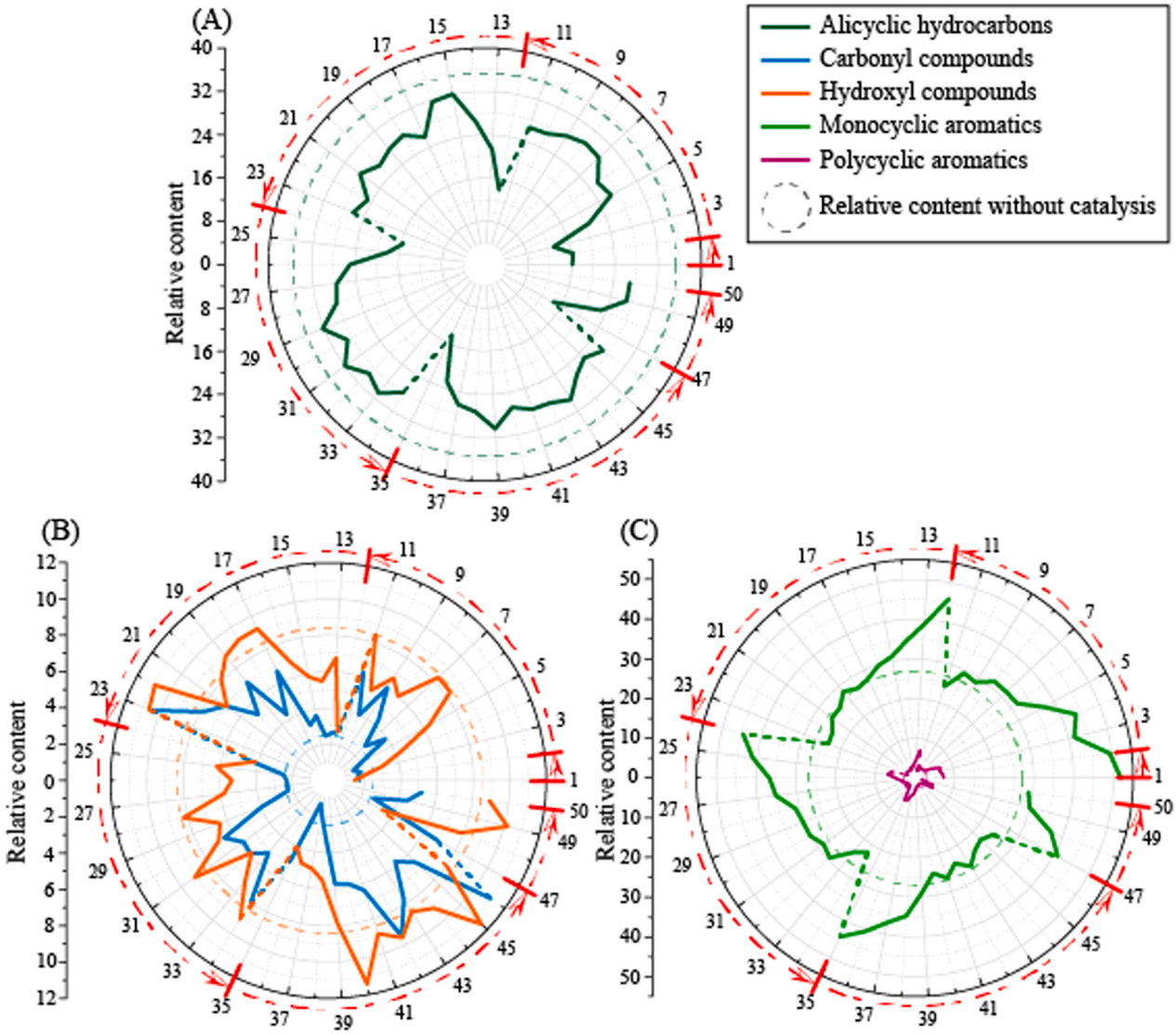

Fig. 7. The composition of condensable organic compounds during pulse pyrolysis of oleic acid.

during the pyrolysis of FFAs through decarboxylation and ketonization. Studies showed that 31% initial oxygen was converted into H_2O during the pyrolysis of oleic acid [52], and 70% for triglyceride [53]. Absorption peaks between 3000 and 2800 cm^{-1} (including 2974 cm^{-1}, 2925 cm^{-1}, 2873 cm^{-1}, and 2854 cm^{-1}) and 1700–1300 cm^{-1} indicated the presence of aromatic C—C bond in the catalyst, which indicated the presence of coke in the catalysts, but the overall absorption peak intensity was very weak. However, overall, the coking was not obvious, and the catalyst deactivation may be mainly caused by the formation of $Ca(OH)_2$ and $CaCO_3$. Fig. 10 showed XRD analysis of the catalyst, CaO, $Ca(OH)_2$, and $CaCO_3$ were the main crystal phases of the catalyst, which was consistent with the result of FT-IR analysis. However, after 50 times of pulse pyrolysis of FFAs, there was still obvious CaO phase in catalyst. Specific content of CaO in the original and used catalysts were calculated according to TG analysis in the following part.

Origin-CaO: Original CaO calcined at 900 °C for 2 h, WCO-CaO: CaO catalyst after 50 times of pulse pyrolysis of WCO, SA-CaO: CaO catalyst after 50 times of pulse pyrolysis of stearic acid, OA-CaO: CaO catalyst after 50 times of pulse pyrolysis of oleic acid, LA-CaO: CaO catalyst after 50 times of pulse pyrolysis of linoleic acid.

TG analysis of catalyst was shown in Fig. 11. The contents of $Ca(OH)_2$ and $CaCO_3$ were calculated based on the mass loss ratio of the catalyst in two different temperature ranges, and the reaction of $Ca(OH)_2 \rightarrow CaO + H_2O$ and $CaCO_3 \rightarrow CaO + CO_2$, which were shown in Table 3. The original CaO was partially hydrated according to the TG analysis. The highest content of $Ca(OH)_2$ in CaO catalyst reached 72.60% after 50 times of pulsed pyrolysis of WCO, and the highest content of $CaCO_3$ in CaO catalyst reached 26.55% after 50 times of pulsed pyrolysis of linoleic acid. The lowest content of CaO was found in WCO-CaO sample, which proved that CaO catalyst had poor regeneration performance at 500 °C during the pulse pyrolysis of WCO (Fig. 5). Different contents of $Ca(OH)_2$ and $CaCO_3$ supported the previous hypothesis (Section 3.2.2 of this paper) that there were different deoxygenation pathways of WCO and FFAs. More H_2O was generated in the pyrolysis process of WCO. H_2O in the product promotes the formation of $CaCO_3$ in the internal of CaO particles [49]. This may cause the $Ca(OH)_2$ to be coated with $CaCO_3$, which inhibits the decomposition of $Ca(OH)_2$ at 500 °C temperatures in this study. As showed in Fig. 5, the activity of catalyst hardly recovered during the pulse pyrolysis of WCO is consistent with the speculation. The promotion pathway of the $CaCO_3$ formation in the internal of CaO by the presence of H_2O is described as follows. Specifically, the H_2O first dissociates to OH^- and H^+ catalyzed by CaO. H^+ attack CaO to form OH^- and Ca^+. At the same time, OH^- will form O^{2-} and H^+ under the action of CaO. And O^{2-} reacts with CO_2 to form CO_3^{2-}, further forming $CaCO_3$. The diameter of H_2O is smaller than that of CO_2 [54], so it is easier for the H_2O to enter the inside of the CaO particles,

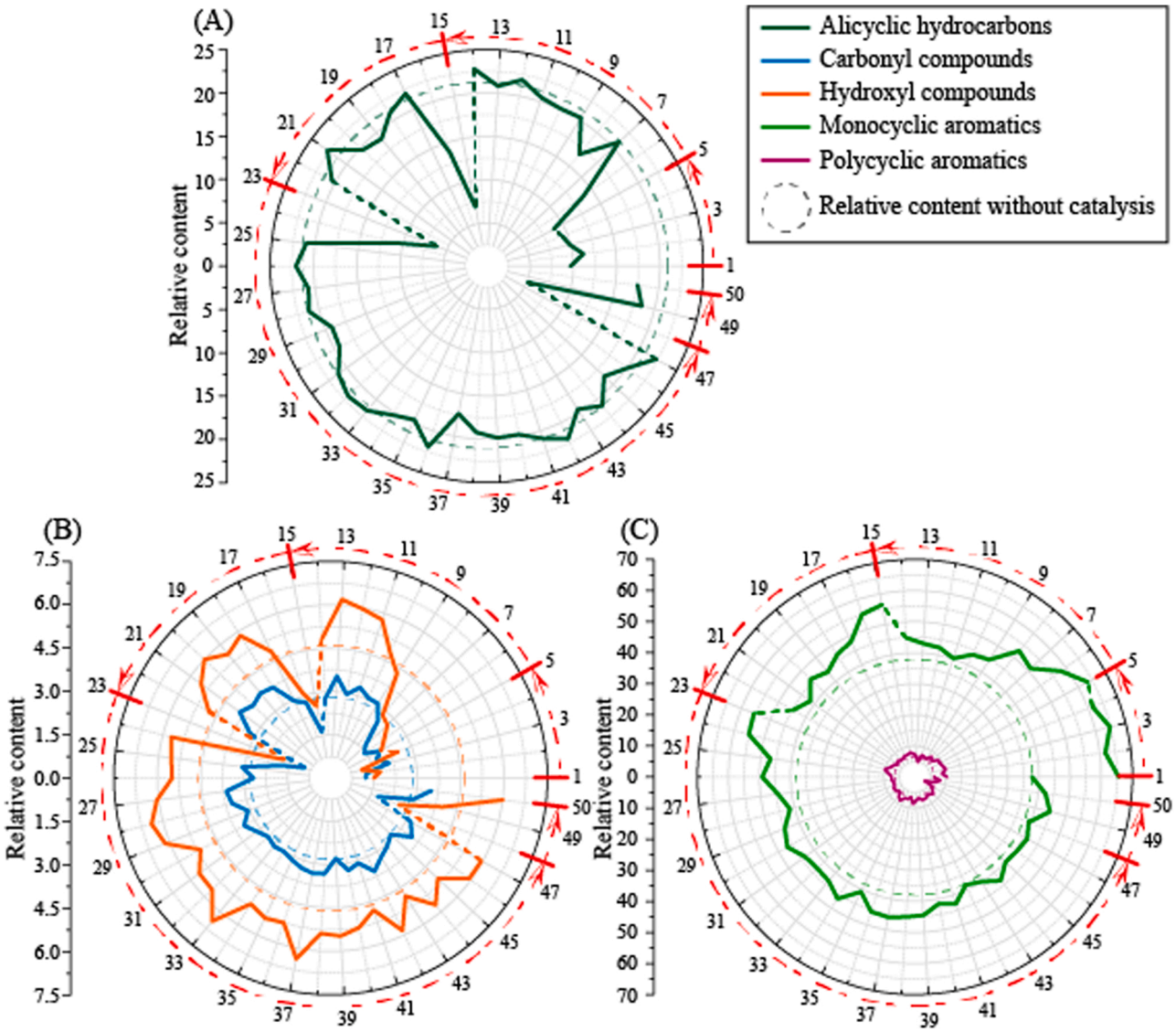

Fig. 8. The composition of condensable organic compounds during pulse pyrolysis of linoleic acid.

and the H^+ formed on the interface are easier to enter the CaO particles. This disrupts the structure of CaO particles and encourages the entry of CO_2, which promotes the formation of $CaCO_3$ in the internal of CaO particles. The TG analysis of the used-CaO (WCO-CaO, SA-CaO, OA-CaO, and LA-CaO) showed that no obvious coke was produced on the surface of catalyst. This could be because basic sites of catalyst could restrain the formation of coke [46,47]. At the same time, compared with lignocellulosic biomass, there was no aromatic ring structure in lipid biomass, which was not easy to cause the catalyst coking, because the precursors of coke were mainly aromatics.

GC/MS analysis of CH_2Cl_2 extraction solution showed that there were no soluble organic compounds on the used-CaO (Supplement date, Fig. S3). The results were consisted with the TG analysis of the used-CaO. Previous studies about the deactivation of acidic catalysts (such as ZSM-5, activated carbon) showed that two types of coke were detected on ZSM-5, and the main culprit of catalyst deactivation was coking [55–57]. The basic sites of CaO catalyst could inhibit the further formation of polycyclic aromatics and coke [47,58]. At the same time, the characteristics of feedstock had a significant influence on the deactivation of catalyst. On the one hand, no aromatic ring structure compounds existed in lipid biomass, which reduced the formation of coke. On the other hand, the formation of CO_2 during the pyrolysis of lipid biomass could react with coke to eliminate coke deposited on catalyst [59].

Characterization of used-catalysts showed that the deactivation of catalyst is mainly caused by the change of crystal phases and agglomeration. CO_2, H_2O and acid produced during the catalytic pyrolysis are the main compounds leading to crystal phase change. Also, the agglomeration of used catalysts was observed according to the particle size and SEM analysis of fresh and used catalysts. Catalyst agglomeration limits gas diffusion and leads to faster deactivation rate. The presence of H_2O promotes the particle internal diffusion of CO_2 [49], leading to particle morphology change and an appearance of physical damage (as shown in Fig. S1). This agrees with the results of SEM morphology and the highest $CaCO_3$ content of 26.55% in LA-CaO, so the damage properties of the catalyst particles were stronger than the other. Such damage was irreversible, and it led to more severe agglomeration of the used catalyst, which is consisted with the particle size and SEM analysis. It accelerated the rate of catalyst deactivation after regeneration. This inference is consistent with the results of the previous experimental results of accelerated deactivation rate (3.2.2 Pulse pyrolysis with CaO catalyst). In the following research, the CaO catalyst can be modified or blended with other metal oxides to improve its hydration resistance and agglomeration resistance to prolong its service life. For the industrial

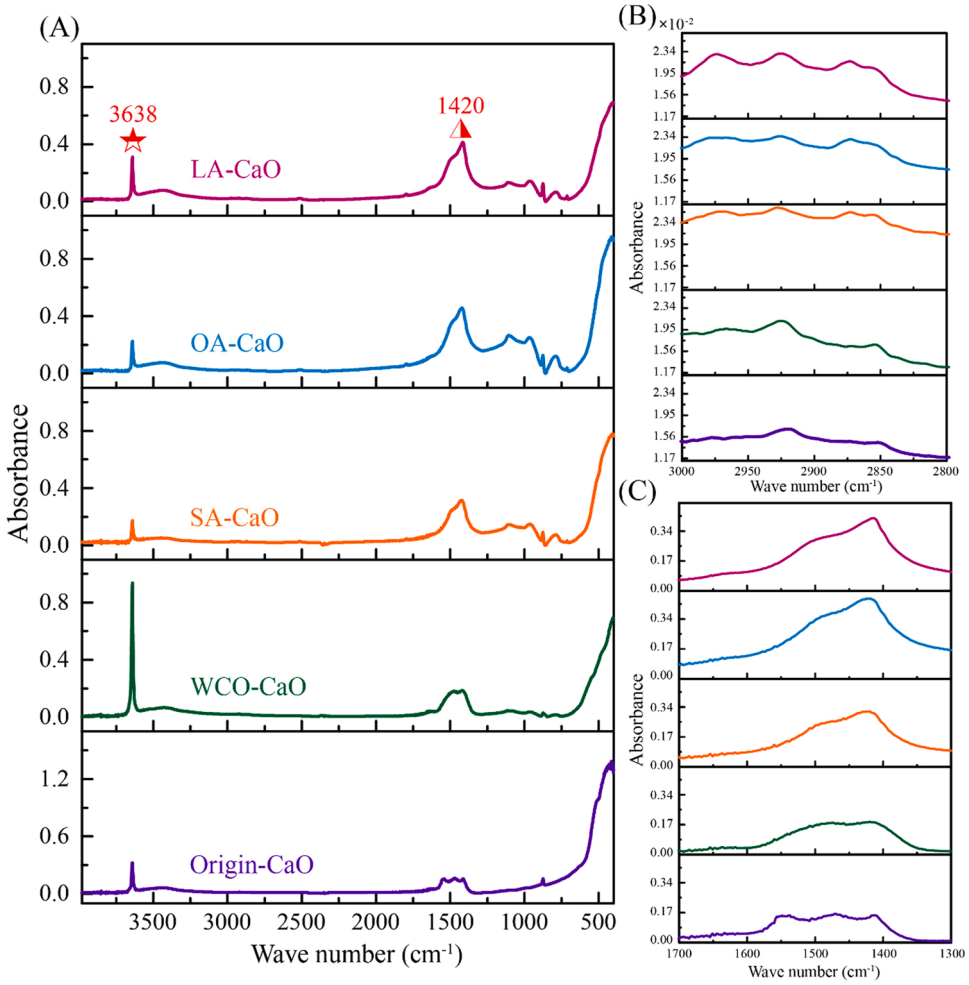

Fig. 9. The FT-IR analysis of the origin-CaO and used CaO. (A) the complete FTIR spectra; (B) 2800–3000 cm-1 bands associated with aromatic C-C bond; (C) 1300–1700 cm-1 bands associated with aromatic C-C bond.

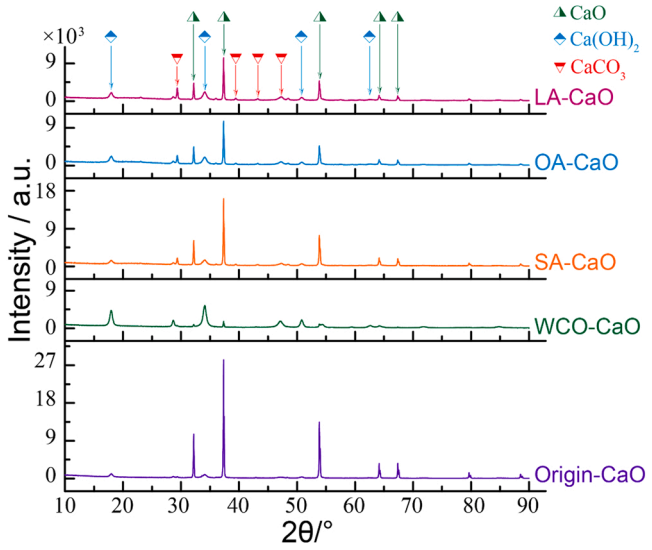

Fig. 10. The XRD analysis of the origin-CaO and used CaO. Origin-CaO: Original CaO calcined at 900 °C for 2 h, WCO-CaO: CaO catalyst after 50 times of pulse pyrolysis of WCO, SA-CaO: CaO catalyst after 50 times of pulse pyrolysis of stearic acid, OA-CaO: CaO catalyst after 50 times of pulse pyrolysis of oleic acid, LA-CaO: CaO catalyst after 50 times of pulse pyrolysis of linoleic acid.

application in the future, it can be considered to design an online regeneration process to reduce the production line downtime, since Ca $(OH)_2$ can be calcined at high temperature to CaO. However, the effect of regeneration on the catalytic activity of CaO catalyst, including the active site and pore structure, cannot be ignored, which needs to be considered in subsequent studies.

4. Conclusion

Combined with the pyrolysis characteristics of WCO and three kinds of FFAs, the deactivation behavior of CaO catalyst during pulse pyrolysis of WCO and FFAs was studied in real-time. The main reasons for CaO catalyst deactivation during the pyrolysis of WCO were investigated, which provided an effective basic data for improving the service life of CaO catalyst.

The results showed that pyrolysis temperature of WCO was about 150 °C higher than that of FFAs. The initial decomposition temperature of FFAs decreased due to the effect of C-C double bond. At the same time, the presence of C-C double bond significantly reduced the amounts of oxygen-contain compounds in the COCs. CaO showed catalytic activity not only for the deoxygenation of carboxyl compounds, but also for hydroxyl compounds and carbonyl compounds. CaO catalyst was completely deactivated after several times of pulse pyrolysis for WCO catalyst pyrolysis. The first complete deactivation time of CaO catalyst in the process of catalytic pyrolysis of FFAs was longer than that of WCO. During the pyrolysis of WCO, the catalytic activity of CaO did not recover after the pause of pulse pyrolysis over 10 h. However, the

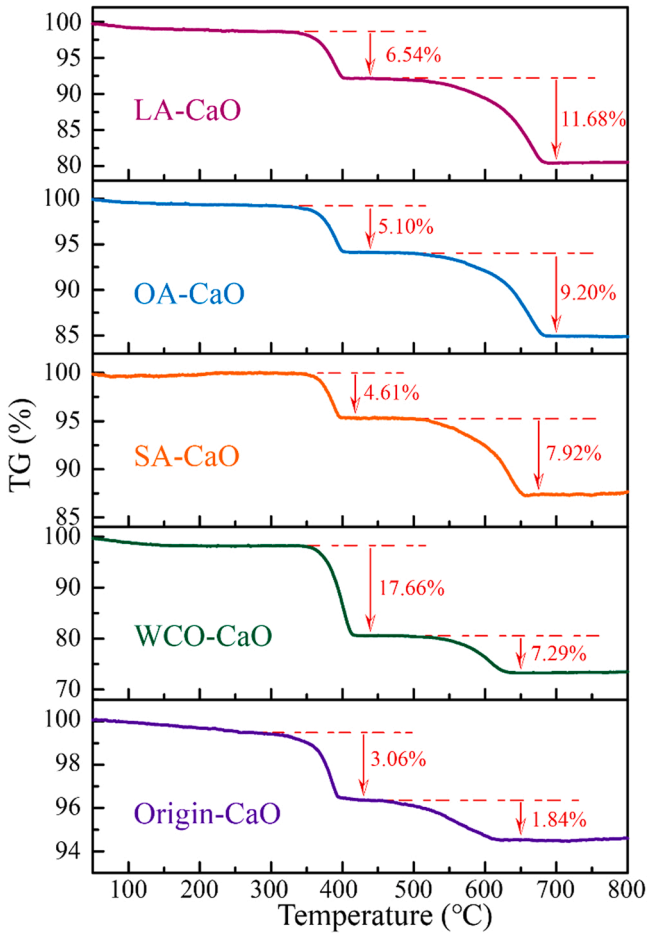

Fig. 11. The TG analysis of the origin-CaO and used CaO. Origin-CaO: Original CaO calcined at 900 °C for 2 h, WCO-CaO: CaO catalyst after 50 times of pulse pyrolysis of WCO, SA-CaO: CaO catalyst after 50 times of pulse pyrolysis of stearic acid, OA-CaO: CaO catalyst after 50 times of pulse pyrolysis of oleic acid, LA-CaO: CaO catalyst after 50 times of pulse pyrolysis of linoleic acid.

Table 3
The special content of CaO, $Ca(OH)_2$, and $CaCO_3$ in the catalysts.

	CaO	Ca $(OH)_2$	$CaCO_3$
Origin-CaO	83.24%	12.58%	4.18%
WCO-CaO	10.83%	72.60%	16.57%
SA-CaO	63.05%	18.95%	18.00%
OA-CaO	58.12%	20.97%	20.91%
LA-CaO	46.56%	26.89%	26.55%

catalytic activity all recovered during the pyrolysis of three FFAs after regeneration, but then the rate of deactivation was accelerated. A large amount of $Ca(OH)_2$ and $CaCO_3$ were detected in the deactivated catalyst, and soluble coke was not detected. The content of $Ca(OH)_2$ in CaO catalyst reached 72.60% after 50 times of pulsed pyrolysis of WCO. The deoxygenation pathways of WCO and FFAs were different during catalytic pyrolysis, and more H_2O was generated in the pyrolysis process of WCO, which promotes the formation of $CaCO_3$ in the internal of CaO particles. This study suggests that the change of crystal phases and agglomeration were the vital cause of CaO deactivation. And the change of morphology affects the regeneration performance of used catalysts. This study provides direction for the subsequent catalyst modification. In the following research, the CaO catalyst can be modified or blended with other metal oxides to improve its hydration resistance and prolong its service life.

CRediT authorship contribution statement

Qiuhao Wu: Conceptualization, Writing – review & editing, Funding acquisition. **Linyao Ke:** Conceptualization, Investigation, Project administration. **Yunpu Wang:** Funding acquisition, Supervision, Project administration. **Nan Zhou:** Writing – review & editing. **Hui Li:** Writing – review & editing. **Qi Yang:** Data Curation, Writing – original draft. **Jiamin Xu:** Resources. Writing – original draft. **Leilei Dai:** Writing – original draft. **Rongge Zou:** Writing – review & editing. **Yuhuan Liu:** Supervision, Funding acquisition, Validation. **Roger Ruan:** Supervision, Project administration.

Declaration of Competing Interest

The authors declare that they have no known competing financial interests or personal relationships that could have appeared to influence the work reported in this paper.

Acknowledgements

This project was financially supported by the National Natural Science Foundation of China (No. 21766019); (No. 21878137), The Centrally Guided Local Science Technology Special Project (20202ZDB01012), The Major Discipline Academic and Technical Leaders Training Program of Jiangxi Province (20204BCJ23011), Graduate Student Innovation Project of Jiangxi Province (YC2020-S005).

Appendix A. Supporting information

Supplementary data associated with this article can be found in the online version at doi:10.1016/j.apcatb.2021.120968.

References

[1] H. Li, H. Chu, X. Ma, G. Wang, F. Liu, M. Guo, W. Lu, S. Zhou, M. Yu, Efficient heterogeneous acid synthesis and stability enhancement of UiO-66 impregnated with ammonium sulfate for biodiesel production, Chem. Eng. J. 408 (2021), 127277.
[2] X. Yao, T.J. Strathmann, Y. Li, L.E. Cronmiller, H. Ma, J. Zhang, Catalytic hydrothermal deoxygenation of lipids and fatty acids to diesel-like hydrocarbons: a review, Green Chem. 23 (2021) 1114–1129.
[3] M. Guiyuan, T. Zhouyi, Z. Xingguo, Z. Jing, Development strategy and analysis of production and consumption demand of plant oilseeds and oils in china, China Oils Fats 45 (2020) 1–4+27 (in chinese).
[4] V. Paasikallio, C. Lindfors, E. Kuoppala, Y. Solantausta, A. Oasmaa, J. Lehto, J. Lehtonen, Product quality and catalyst deactivation in a four day catalytic fast pyrolysis production run, Green Chem. 16 (2014) 3549.
[5] B. Al Alwan, S.O. Salley, K.Y.S. Ng, Biofuels production from hydrothermal decarboxylation of oleic acid and soybean oil over Ni-based transition metal carbides supported on Al-SBA-15, Appl. Catal. A Gen. 498 (2015) 32–40.
[6] X. Li, X. Luo, Y. Jin, J. Li, H. Zhang, A. Zhang, J. Xie, Heterogeneous sulfur-free hydrodeoxygenation catalysts for selectively upgrading the renewable bio-oils to second generation biofuels, Renew. Sustain. Energy Rev. 82 (2018) 3762–3797.
[7] Q. Wu, Y. Wang, Y. Peng, L. Ke, Q. Yang, L. Jiang, L. Dai, Y. Liu, R. Ruan, D. Xia, L. Jiang, Microwave-assisted pyrolysis of waste cooking oil for hydrocarbon bio-oil over metal oxides and HZSM-5 catalysts, Energy Convers. Manag. 220 (2020), 113124.
[8] W. Yinhui, Z. Rong, Q. Yanhong, P. Jianfei, L. Mengren, L. Jianrong, W. Yusheng, H. Min, S. Shijin, The impact of fuel compositions on the particulate emissions of direct injection gasoline engine, Fuel 166 (2016) 543–552.
[9] J. Xu, F. Long, J. Jiang, F. Li, Q. Zhai, F. Wang, P. Liu, J. Li, Integrated catalytic conversion of waste triglycerides to liquid hydrocarbons for aviation biofuels, J. Clean. Prod. 222 (2019) 784–792.
[10] H. Seifi, S.M. Sadrameli, Improvement of renewable transportation fuel properties by deoxygenation process using thermal and catalytic cracking of triglycerides and their methyl esters, Appl. Therm. Eng. 100 (2016) 1102–1110.
[11] A. Bayat, S.M. Sadrameli, Production of renewable aromatic hydrocarbons via conversion of canola oil methyl ester (CME) over zinc promoted HZSM-5 catalysts, Renew. Energy 106 (2017) 62–67.
[12] J. Grams, A.M. Ruppert, Catalyst stability—bottleneck of efficient catalytic pyrolysis, Catalysts 11 (2021) 265.
[13] Y. Wang, Q. Wu, S. Yang, Q. Yang, J. Wu, Z. Ma, L. Jiang, Z. Yu, L. Dai, Y. Liu, R. Ruan, G. Fu, B. Zhang, H. Zhu, Microwave-assisted catalytic fast pyrolysis

coupled with microwave-absorbent of soapstock for bio-oil in a downdraft reactor, Energy Convers. Manag. 185 (2019) 11–20.
[14] J. Fu, J. Zhang, C. Jin, Z. Wang, T. Wang, X. Cheng, C. Ma, Effects of temperature, oxygen and steam on pore structure characteristics of coconut husk activated carbon powders prepared by one-step rapid pyrolysis activation process, Bioresour. Technol. 310 (2020), 123413.
[15] H. Li, Y. Wang, X. Ma, Z. Wu, P. Cui, W. Lu, F. Liu, H. Chu, Y. Wang, A novel magnetic CaO-based catalyst synthesis and characterization: enhancing the catalytic activity and stability of CaO for biodiesel production, Chem. Eng. J. 391 (2020), 123543.
[16] K.G. Kalogiannis, S.D. Stefanidis, S.A. Karakoulia, K.S. Triantafyllidis, H. Yiannoulakis, C. Michailof, A.A. Lappas, First pilot scale study of basic vs acidic catalysts in biomass pyrolysis: deoxygenation mechanisms and catalyst deactivation, Appl. Catal. B Environ. 238 (2018) 346–357.
[17] L. Yi, H. Liu, M. Li, G. Man, H. Yao, Prevention of CaO deactivation using organic calcium precursor during multicyclic catalytic upgrading of bio-oil, Fuel 271 (2020), 117692.
[18] Y. Fan, Y. Cai, X. Li, H. Yin, J. Xia, Coking characteristics and deactivation mechanism of the HZSM-5 zeolite employed in the upgrading of biomass-derived vapors, J. Ind. Eng. Chem. 46 (2017) 139–149.
[19] H. Li, Y. Xu, C. Gao, Y. Zhao, Structural and textural evolution of Ni/γ-Al2O3 catalyst under hydrothermal conditions, Catal. Today 158 (2010) 475–480.
[20] J. Sehested, J.A.P. Gelten, S. Helveg, Sintering of nickel catalysts: effects of time, atmosphere, temperature, nickel-carrier interactions, and dopants, Appl. Catal. A Gen. 309 (2006) 237–246.
[21] F. Bimbela, J. Ábrego, R. Puerta, L. García, J. Arauzo, Catalytic steam reforming of the aqueous fraction of bio-oil using Ni-Ce/Mg-Al catalysts, Appl. Catal. B Environ. 209 (2017) 346–357.
[22] S.D. Stefanidis, K.G. Kalogiannis, P.A. Pilavachi, C.M. Fougret, E. Jordan, A. A. Lappas, Catalyst hydrothermal deactivation and metal contamination during the in situ catalytic pyrolysis of biomass, Catal. Sci. Technol. 6 (2016) 2807–2819.
[23] Y. Qiao, B. Wang, P. Zong, Y. Tian, F. Xu, D. Li, F. Li, Y. Tian, Thermal behavior, kinetics and fast pyrolysis characteristics of palm oil: analytical TG-FTIR and Py-GC/MS study, Energy Convers. Manag. 199 (2019), 111964.
[24] E. Kozliak, M. Sulkes, I.P. Smoliakova, I. Alhroub, B. Nespor, B. Yao, A. Kubatova, Pathways toward PAH formation during fatty acid and triglyceride pyrolysis, J. Phys. Chem. A 124 (2020) 7559–7574.
[25] A. Kubátová, J. Šťávová, W.S. Seames, Y. Luo, S.M. Sadrameli, M.J. Linnen, G. V. Baglayeva, I.P. Smoliakova, E.I. Kozliak, Triacylglyceride thermal cracking: pathways to cyclic hydrocarbons, Energy Fuels 26 (2011) 672–685.
[26] F. Long, Q. Zhai, P. Liu, X. Cao, X. Jiang, F. Wang, L. Wei, C. Liu, J. Jiang, J. Xu, Catalytic conversion of triglycerides by metal-based catalysts and subsequent modification of molecular structure by ZSM-5 and Raney Ni for the production of high-value biofuel, Renew. Energy 157 (2020) 1072–1080.
[27] T. Thangadurai, C.T. Tye, Acidity and basicity of metal oxide-based catalysts in catalytic cracking of vegetable oil, Braz. J. Chem. Eng. 38 (2021) 1–20.
[28] A. Arregi, M. Amutio, G. Lopez, M. Artetxe, J. Alvarez, J. Bilbao, M. Olazar, Hydrogen-rich gas production by continuous pyrolysis and in-line catalytic reforming of pine wood waste and HDPE mixtures, Energy Convers. Manag. 136 (2017) 192–201.
[29] J. Alvarez, S. Kumagai, C. Wu, T. Yoshioka, J. Bilbao, M. Olazar, P.T. Williams, Hydrogen production from biomass and plastic mixtures by pyrolysis-gasification, Int. J. Hydrog. Energy 39 (2014) 10883–10891.
[30] T. Suprianto, Winarto, W. Wijayanti, I.N.G. Wardana, Synergistic effect of curcumin and activated carbon catalyst enhancing hydrogen production from biomass pyrolysis, Int. J. Hydrog. Energy 46 (2021) 7147–7164.
[31] Y. Wen, Y. Xie, C. Jiang, W. Li, Y. Hou, Products distribution and interaction mechanism during co-pyrolysis of rice husk and oily sludge by experiments and reaction force field simulation, Bioresour. Technol. 329 (2021), 124822.
[32] S. Pourkarimi, A. Hallajisani, A. Alizadehdakhel, A. Nouralishahi, Biofuel production through micro- and macroalgae pyrolysis – a review of pyrolysis methods and process parameters, J. Anal. Appl. Pyrolysis 142 (2019), 104599.
[33] H. Kawamoto, T. Watanabe, S. Saka, Strong interactions during lignin pyrolysis in wood – A study by in situ probing of the radical chain reactions using model dimers, J. Anal. Appl. Pyrolysis 113 (2015) 630–637.
[34] T. Kotake, H. Kawamoto, S. Saka, Mechanisms for the formation of monomers and oligomers during the pyrolysis of a softwood lignin, J. Anal. Appl. Pyrolysis 105 (2014) 309–316.
[35] L. Xu, J.-H. Cheng, P. Liu, Q. Wang, Z.-X. Xu, Q. Liu, J.-Y. Shen, L.-J. Wang, Production of bio-fuel oil from pyrolysis of plant acidified oil, Renew. Energy 130 (2019) 910–919.
[36] H. Yuan, H. Fan, R. Shan, M. He, J. Gu, Y. Chen, Study of synergistic effects during co-pyrolysis of cellulose and high-density polyethylene at various ratios, Energy Convers. Manag. 157 (2018) 517–526.
[37] T.N. Pham, T. Sooknoi, S.P. Crossley, D.E. Resasco, Ketonization of carboxylic acids: mechanisms, catalysts, and implications for biomass conversion, ACS Catal. 3 (2013) 2456–2473.
[38] J. Gupta, K. Papadikis, E.Y. Konysheva, Y. Lin, I.V. Kozhevnikov, J. Li, CaO catalyst for multi-route conversion of oakwood biomass to value-added chemicals and fuel precursors in fast pyrolysis, Appl. Catal. B Environ. 285 (2021), 119858.
[39] M. Argyle, C. Bartholomew, Heterogeneous catalyst deactivation and regeneration: a review, Catalysts 5 (2015) 145–269.
[40] J. Zhou, J. Zhao, J. Zhang, T. Zhang, M. Ye, Z. Liu, Regeneration of catalysts deactivated by coke deposition: a review, Chin. J. Catal. 41 (2020) 1048–1061.
[41] S. Kumagai, R. Yamasaki, T. Kameda, Y. Saito, A. Watanabe, C. Watanabe, N. Teramae, T. Yoshioka, Aromatic hydrocarbon selectivity as a function of CaO basicity and aging during CaO-catalyzed PET pyrolysis using tandem μ-reactor-GC/MS, Chem. Eng. J. 332 (2018) 169–173.
[42] S. Kumagai, R. Yamasaki, T. Kameda, Y. Saito, A. Watanabe, C. Watanabe, N. Teramae, T. Yoshioka, Tandem μ-reactor-GC/MS for online monitoring of aromatic hydrocarbon production via CaO-catalysed PET pyrolysis, React. Chem. Eng. 2 (2017) 776–784.
[43] A.M. Ruppert, J.D. Meeldijk, B.W. Kuipers, B.H. Erne, B.M. Weckhuysen, Glycerol etherification over highly active CaO-based materials: new mechanistic aspects and related colloidal particle formation, Chem. Eur. J. 14 (2008) 2016–2024.
[44] M. Calatayud, A.M. Ruppert, B.M. Weckhuysen, Theoretical study on the role of surface basicity and lewis acidity on the etherification of glycerol over alkaline earth metal oxides, Chem. Eur. J. 15 (2009) 10864–10870.
[45] C. Liu, H. Wang, A.M. Karim, J. Sun, Y. Wang, Catalytic fast pyrolysis of lignocellulosic biomass, Chem. Soc. Rev. 43 (2014) 7594–7623.
[46] N. Asikin-Mijan, H.V. Lee, J.C. Juan, A.R. Noorsaadah, H.C. Ong, S.M. Razali, Y. H. Taufiq-Yap, Promoting deoxygenation of triglycerides via Co-Ca loaded SiO_2 -Al_2O_3 catalyst, Appl. Catal. A Gen. 552 (2018) 38–48.
[47] G. Abdulkareem-Alsultan, N. Asikin-Mijan, G. Mustafa-Alsultan, H.V. Lee, K. Wilson, Y.H. Taufiq-Yap, Efficient deoxygenation of waste cooking oil over Co_3O_4–La_2O_3-doped activated carbon for the production of diesel-like fuel, RSC Adv. 10 (2020) 4996–5009.
[48] H. Li, Y. Wang, N. Zhou, L. Dai, W. Deng, C. Liu, Y. Cheng, Y. Liu, K. Cobb, P. Chen, R. Ruan, Applications of calcium oxide-based catalysts in biomass pyrolysis/gasification: a review, J. Clean. Prod. 291 (2021), 125826.
[49] N. Wang, Y. Feng, X. Guo, A.C.T. van Duin, Insights into the role of H_2O in the carbonation of CaO nanoparticle with CO_2, J. Phys. Chem. C 122 (2018) 21401–21410.
[50] Z. Hussain, S. Khan, M. Rafiq, M.Y. Naz, N.M. AbdEl-Salam, K.A. Ibrahim, Catalytic valorization of waste soap into hydrocarbon rich oil and fuel gas, Biomass Convers. Biorefinery 10 (2019) 1091–1098.
[51] Y. Wang, Q. Yang, L. Ke, Y. Peng, Y. Liu, Q. Wu, X. Tian, L. Dai, R. Ruan, L. Jiang, Review on the catalytic pyrolysis of waste oil for the production of renewable hydrocarbon fuels, Fuel 283 (2021), 119170.
[52] S. He, F.G.H. Klein, T.S. Kramer, A. Chandel, Z. Tegudeer, A. Heeres, H.J. Heeres, Catalytic conversion of free fatty acids to bio-based aromatics: a model investigation using oleic acid and an H-ZSM-5/Al_2O_3 catalyst, ACS Sustain. Chem. Eng. 9 (2021) 1128–1141.
[53] J.A. Melero, M.M. Clavero, G. Calleja, A. García, Rn Miravalles, T. Galindo, Production of biofuels via the catalytic cracking of mixtures of crude vegetable oils and nonedible animal fats with vacuum gas oil, Energy Fuel 24 (2010) 707–717.
[54] C. Sun, B. Bai, Selective permeation of gas molecules through a two-dimensional graphene nanopore, Acta Phys. Chim. Sin. 34 (2018) 1136–1143.
[55] D. Duan, Y. Zhang, Y. Wang, H. Lei, Q. Wang, R. Ruan, Production of renewable jet fuel and gasoline range hydrocarbons from catalytic pyrolysis of soapstock over corn cob-derived activated carbons, Energy 209 (2020), 118454.
[56] W.-L. Fanchiang, Y.-C. Lin, Catalytic fast pyrolysis of furfural over H-ZSM-5 and Zn/H-ZSM-5 catalysts, Appl. Catal. A Gen. 419 (420) (2012) 102–110.
[57] C.A. Mullen, C. Dorado, A.A. Boateng, Catalytic co-pyrolysis of switchgrass and polyethylene over HZSM-5: catalyst deactivation and coke formation, J. Anal. Appl. Pyrolysis 129 (2018) 195–203.
[58] J. Chen, J. Sun, Y. Wang, Catalysts for steam reforming of bio-oil: a review, Ind. Eng. Chem. Res. 56 (2017) 4627–4637.
[59] C. Di Stasi, D. Alvira, G. Greco, B. González, J.J. Manyà, Physically activated wheat straw-derived biochar for biomass pyrolysis vapors upgrading with high resistance against coke deactivation, Fuel 255 (2019), 115807.